Batteries & Supercaps

Research Article
doi.org/10.1002/batt.202300367

Chemistry Europe
European Chemical Societies Publishing

www.batteries-supercaps.org

Preconditioning Operation of Membraneless Vanadium Micro Redox Flow Batteries

Beatriz Oraá-Poblete,[a, b] Daniel Perez-Antolin,[a] Ange A. Maurice,[c] Jesus Palma,[d] Erik Kjeang,[e] and Alberto E. Quintero*[a, c]

Development of a Membraneless Vanadium Micro Redox Flow Battery (MVMRFB) with an automated closed-loop control, using micro actuators and micro sensors, is presented for the first-time during electrolyte preconditioning operation in recirculation mode. The progress of preconditioning is tracked with UV-vis spectroscopy by 3D printed micro flow cuvettes. Influence of flow rate, reactor internal resistance, and presence of side reactions in the preconditioning process are studied. Optimal flow rate ratio between negative and positive electrolytes is determined and significant performance improvements achieved by operating at lower flow rates are obtained. Influence of reactor internal resistance, which is directly related with the maximum power density, is evaluated demonstrating that operating at a high-power density can be a source of inefficiency due to the presence of side reactions. Finally, presence of side reactions is evaluated through a dual measurement of electrolytes concentrations in both negative and positive side, and it is demonstrated to be a cause for charge imbalance between the two half-cells. This work lays a solid foundation for the successful implementation of a charge-discharge cycle in MVMRFBs operating in recirculation mode.

Introduction

From 1980 onwards, global warming due to climate change generated by anthropogenic means became a cause for environmental concern.[1] In this context, the transition from fossil fuels to renewable energies becomes evident. However, these resources present a weakness regarding seasonality, fluctuations, and dependance on the weather conditions. Addressing these problems requires tools that allow to store energy during periods of high production and release it when production is low. In this regard, the Redox Flow Battery (RFB) is a promising candidate, because it can provide capacity firming services to power grids with high penetration of intermittent renewable sources.

A large body of work has been developed regarding RFB,[2–4] with Vanadium Redox Flow Batteries (VRFB) being the most reliable and mature technology for applications at large scale. Reaction kinetics of these systems are fast and highly reversible, resulting in energy efficiencies as high as 90%. These devices also count on 100% of energy capacity warranted during >10,000 cycles. Moreover, power-related costs have declined significantly due to a number of system improvements, including revisions to the electrolyte chemistry,[5,6] separator technology,[7,8] electrodes improvement[9,10] and increased power density,[11,12] although in these devices the energy density (15–25 Wh L^{-1}) is limited by redox species solubility, since at high concentrations they can precipitate.[13] Moreover, VRFBhas the main advantage of being symmetric systems, which means that the same electrolyte is introduced in both half cells, and it avoids the risk of electrolyte contamination during operation. This advantage brought rapidly the system to the market.

For conventional VRFB, energy conversion takes place in the electrodes of an electrochemical reactor which is divided into two half cells. They are separated from each other by an ion-selective membrane (proton/cation exchange membrane in VRFB), so the advective mixing of their respective electrolytes is avoided while charge balance is ensured, ideally without the negative and positive active materials coming into direct contact with each other. In electrochemical devices, membranes can fail in their task of separating redox species during operation, so that they not only allow protons transportation,

[a] B. Oraá-Poblete, Dr. D. Perez-Antolin, Dr. A. E. Quintero
R&D Department
Micro Electrochemical Technologies S.L.
Avenida Juan Caramuel 1, 28918 Leganés, Madrid (Spain)
E-mail: alberto.quintero@b5tec.com

[b] B. Oraá-Poblete
Departamento de Ingeniería Química Industrial y del Medio Ambiente
Escuela Técnica Superior de Ingenieros Industriales
Universidad Politécnica de Madrid
C/José Gutierrez Abascal, 2, 28006, Madrid (Spain)

[c] Dr. A. A. Maurice, Dr. A. E. Quintero
Departamento de Ingeniería Térmica y de Fluidos
Universidad Carlos III de Madrid
Escuela Politécnica Superior, Universidad Carlos III de Madrid, 28911 Leganés (Spain)

[d] Dr. J. Palma
Electrochemical Processes Unit
IMDEA Energy
Av. Ramón de La Sagra, 3, 28933 Móstoles, Madrid (Spain)

[e] Dr. E. Kjeang
School of Mechatronic Systems Engineering
Simon Fraser University
250-13450 102 Avenue, Surrey, BC-V3T 0A3, (Canada)

Supporting information for this article is available on the WWW under https://doi.org/10.1002/batt.202300367

but also some redox species (cations) could cross through them, leading to self-discharge. Some recent works look for membranes acting as an efficient barrier layer to vanadium species in VRFB applications.[14] Moreover, membranes increase the internal resistance of the cell, which limits current density, reduces energy efficiency, and increases energy consumption and degradation of the system. Consequently, higher production and maintenance costs are supposed for RFB.

The most recent works focus on overcoming these limitations, rethinking the concept of RFB and searching for new advanced redox flow systems that are membrane-free. At the macroscale, some systems based on biphasic immiscible electrolytes have recently been proposed.[15,16] However, at the microfluidics scale, it is also possible to avoid the use of the membrane with miscible liquids.[17–19] Including novel microfluidics concepts towards the architecture of redox flow batteries has been disruptive during the last years.[20] Microfluidics allows to build more compact global modules that can be stacked for scale-up, overcome shunt currents, and have greater surface-volume ratio and reaction rate, thus improving performance.[21] Stokes flow permits the absence of the membrane, so that mixing is controlled by cross-stream diffusion, while reducing production cost. Because diffusion is a relatively slow process, the thickness of this interfacial diffusion layer must remain within a tolerable range.[19,22]

However, these new designs have their caveats. New problems arise from the growth of depletion layers near the electrodes due to the laminar flow of electrolytes, and precise control of the position of the mixing diffusion layer located in the contact region between electrolytes. To overcome these, special cell designs, accurate flow control systems, and electrodes improvements are all engineering challenges that must be addressed.

Ferrigno et al.[23] tested the first prototype of a membraneless Vanadium micro redox flow battery reactor with a single microchannel of rectangular cross section and planar electrodes at the bottom of the microchannel. Innovative three-dimensional architectures employing graphite rod electrodes or flow-through porous electrodes were introduced by Kjeang et al.[24,25]. Lee et al.[26] carried out the first charge-discharge cycle in a membraneless cell. A significant improvement of their design with respect to previous ones was the recollection of the anolyte and catholyte streams through separated ducts at the outlet of the microchannel. Goulet et al.[17] obtained a reactor with high discharge power densities through an optimized design with carbon nanotubes in the electrolyte solutions but did not attempt in-situ charging.

Membraneless micro RFBs have so far only been demonstrated as single reactor prototypes, without being fully integrated into a microfluidic system. They are most commonly designed as a primary battery or a fuel cell (only discharging) rather than a rechargeable RFB, due to the complexity of the microfluidic pumping system and flow rate control in a continuous operating mode.

Commercial vanadium electrolyte is generally supplied as a 50:50 mixture of V^{3+}/VO^{2+} (or $V^{3.5+}$). Indeed, before starting with charge-discharge cycles of the VRFB, a pre-charge of the battery must be done, which is known as preconditioning phase. During preconditioning, reactions taking place in the positive and negative half-cells are:

$$\text{Positive}: \quad VO^{2+} + V^{3+} + H_2O \rightarrow 2\ VO^{2+} + e^- + 2\ H^+ \tag{1}$$

$$\text{Negative}: \quad VO^{2+} + V^{3+} + e^- + 2\ H^+ \rightarrow 2V^{3+} + H_2O \tag{2}$$

As Equations (1) and (2) show, after the preconditioning, the anolyte is formed by V^{3+} ions and the catholyte by VO^{2+} ions[27] corresponding to state of charge zero for the VRFB. As a first step towards developing rechargeable MVMRFBs, this study focuses on the in-situ preconditioning operation. Although investigation of this step has been frequently ignored in the broader RFB literature, the present work shows that preconditioning has significant influence on the performance of the MVMRFB.

In this work the development of a complete miniaturized MVMRFB, including the reactor and the fluidic system at the microscale, is presented for the first time, overcoming the issues related with microfluidic flow rate control and working in recirculation mode during operation. Micro flow control system components, such as actuators, sensors, and cuvettes to continuously monitor V^{3+} and VO^{2+} relative concentration ratios in the negative and positive electrolytes via UV-visible spectroscopy are used. Preconditioning operation of the MVMRFB is carried out, where the influence of various parameters such as flow rate and reactor power density on the performance is assessed.

Results and Discussion

Influence of operational parameters in preconditioning of MVMRFB

Conventional RFBs, due to the presence of a membrane separating the positive and negative electrolytes, operate in the turbulent flow regime in order to overcome mass transfer limitations. Therefore, working at the same flow rate in both half cells is a common practice that simplifies the flow control algorithms. Moreover, higher flow rates are associated with higher current densities because overpotential is reduced due to constant provision of active species at the electrode surface. The flow rate must however be balanced against parasitic pumping power requirements.

In membraneless micro RFBs, laminar flow is required to facilitate a stable liquid-liquid interface in the absence of membrane, which imposes mass transport limitations, affecting electrochemical performance. In order to overcome mass transport limitations in the MVMRFB, four operational cases are studied during preconditioning, which shed some light on the basic knowledge of how to operate a MVMRFB from fluid dynamics and electrochemical points of view.

Influence of the electrolyte flow rate ratio. Without membrane, the interface between the electrolytes must be accurately controlled to avoid an electrolyte being in direct

Research Article
doi.org/10.1002/batt.202300367
Chemistry Europe
European Chemical Societies Publishing

contact with its opposite electrode. To ensure correct electrochemical performance, an initial assumption is to position the interface at the center of the microchannel.

Preconditioning operation is evaluated at four different flow rate ratios between the negative and positive electrolytes in order to compensate the slower kinetics of negative half-cell reactions and mass transfer limitations. The base case applies equal flow rates for negative and positive electrolytes ($Q_{neg}/Q_{pos}=1$ ratio) of 10 μL/min. Then, the negative flow rate is increased in each preconditioning process to 30 μL/min, 60 μL/min, and 80 μL/min, to obtain Q_{neg}/Q_{pos} ratios of 3, 6, and 8, respectively. The preconditioning progress is monitored through VO^{2+} concentration variations in each stream, measured with the UV-vis spectrometer as per the calibration method described in the Supporting Information. Results are reported in mole fractions, which equivalate to $X_{V^{3+}}$ and $X_{VO^{2+}}$ for the negative and positive half-cells, respectively, starting with the as-received commercial electrolyte with $X_{V^{3+}} = X_{VO^{2+}} = 50\,\%$. At the end of the preconditioning operation, the negative electrolyte will contain surplus V^{3+} while the positive electrolyte will contain surplus VO^{2+}, targeting $X_{V^{3+}} = X_{VO^{2+}} = 100\,\%$.

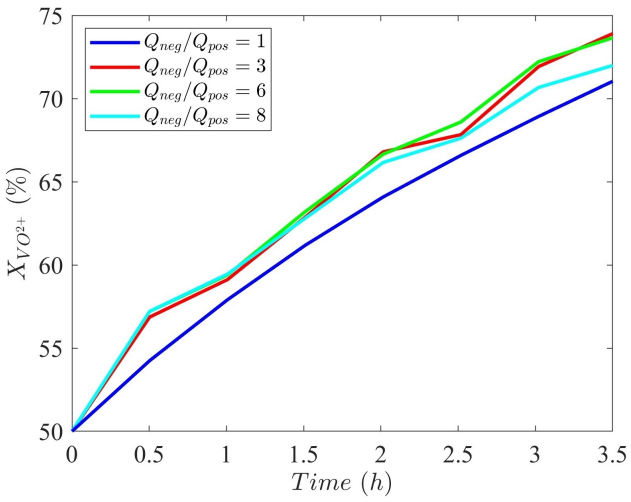

Figure 1. Flow rate ratio influence on $X_{VO^{2+}}$ in the positive electrolyte at constant 1.7 V cell potential for 3.5 h.

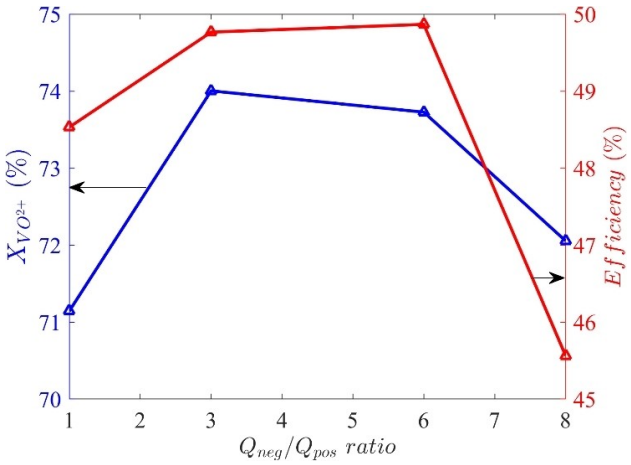

Figure 2. Flow rate ratio influence on final $X_{VO^{2+}}$ (blue line) and process efficiency (red line) at constant 1.7 V.

Preconditioning operation is carried out by applying 1.7 V in potentiostatic mode, with a mean power density of 14 mW/cm^2.

Figure 1 shows $X_{VO^{2+}}$ (at the positive side) as a function of time for several Q_{neg}/Q_{pos} values. The observed trend shows that equal flow rates is not an optimal ratio. When the negative flow rate is increased with respect to positive flow rate, the $X_{VO^{2+}}$ tends to increase due to continuous and faster renewal of species at the electrode surface, thus increasing mass transfer and compensating its apparently slower reaction rate.

Figure 2 shows $X_{VO^{2+}}$ at the final operation time of 3.5 h. The data indicates that a maximum $X_{VO^{2+}}$ is obtained for a $Q_{neg}/Q_{pos}=3$ ratio. Increasing indefinitely the flow rate of negative electrolyte, thus increasing the flow rate ratio, appears to hinder the preconditioning process, possibly caused by, this time, the positive electrolyte acting as the limiting reagent. Figure 2 also shows the efficiency of preconditioning operation, which is calculated based on the final VO^{2+} concentration obtained (effective coulombs determined by spectrometry in the positive electrolyte), divided by the total coulombs supplied by potentiostat in the whole preconditioning process of 3.5 h, for each flow rate ratio. For $Q_{neg}/Q_{pos}=3$ and $Q_{neg}/Q_{pos}=6$ efficiencies are similar, around 50 %, while $X_{VO^{2+}}$ percentages are approximately 74 %. $Q_{neg}/Q_{pos}=3$ is selected as an optimal ratio for the following sections. For more information, current density as a function of time is presented in Figure S4, where it is worth noting that, for equal flow rates ($Q_{neg}/Q_{pos}=1$), the lowest current density is obtained.

Influence of absolute flow rate for a ratio $Q_{neg}/Q_{pos}=3$. Conventional VRFB typically operate at high flow rates in order to decrease local mass transfer concentration overpotential, allowing higher current density and minimizing side reactions.[28]

For fuel cell mode operation with MVMRFB, previous research determined that higher flow rates are related with higher power and current densities, in the same way as conventional VRFB.[25] Nevertheless, flow rate influence remains unexplored in recirculation mode for MVMRFB. With this aim, using the optimal flow rate ratio of $Q_{neg}/Q_{pos}=3$ from the previous section, a 7 h preconditioning operation was carried out with a mean power density of 14 mW/cm^2, operating in potentiostatic mode at 1.7 V. Three different flow rate values at the positive electrolyte of 10 μL/min, 30 μL/min, and 40 μl/min were applied, while continuously measuring the $X_{VO^{2+}}$ with the UV-vis spectrometer.

Figure 3 shows the evolution of $X_{VO^{2+}}$ with time. Contrary to conventional VRFB or MVMRFB in fuel cell mode operation, when battery recirculation mode is applied for MVMRFB, lower flow rates allow to achieve higher values of preconditioning in less time.

Figure 4 shows the final $X_{VO^{2+}}$ for the three studied cases and their efficiencies, as defined in the previous section. Not only the final $X_{VO^{2+}}$ decreases when increasing the flow rates, but also the efficiency drastically decreases from 41 % to 12 %.

Research Article
doi.org/10.1002/batt.202300367
Chemistry Europe
European Chemical Societies Publishing

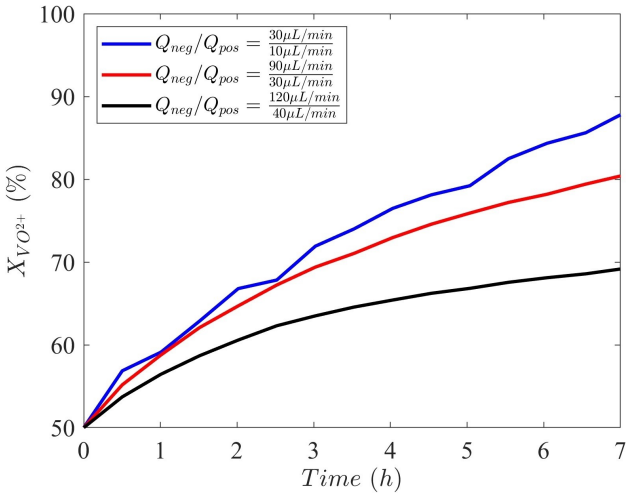

Figure 3. Influence of absolute flow rate in $X_{VO^{2+}}$ for a preconditioning operation at constant 1.7 V with $Q_{neg}/Q_{pos} = 3$ ratio.

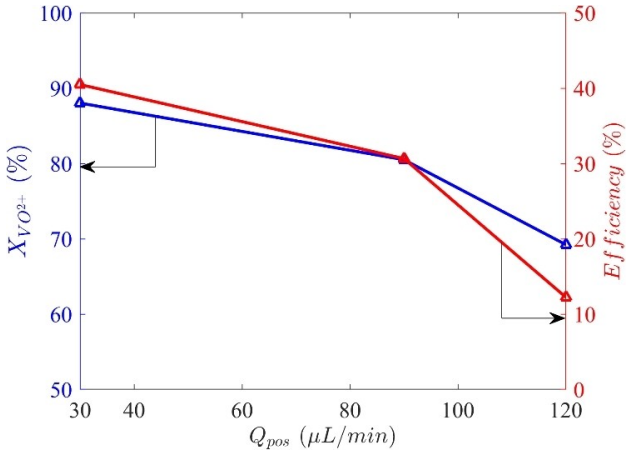

Figure 4. Final $X_{VO^{2+}}$ (blue line) for 7 h operation and efficiency (red line) for different positive flow rates and constant $Q_{neg}/Q_{pos} = 3$ ratio.

Therefore, the results suggest that operating at lower flow rates implies better performance of MVMRFB in recirculation mode, which is directly related with a higher conversion efficiency. At lower flow rates, the electrolytes travel slower through the liquid-liquid interface in the center microchannel, which can increase width of mixing boundary layer, increasing crossover of V^{3+} and VO^{2+}. However, species conversion in one single pass operating at these lower flow rates compensates diffusive mixing.

Higher flow rates are related with a small conversion in one pass and lower efficiencies, even when power and current densities increase.[25] It can be seen in Figure S5 that the current density for this preconditioning operation is doubled for higher flow rates compared with lower flow rates, but the efficiency is decreased from 41% for lower flow rates to 12% for higher flow rates. Finally, mixing boundary layer broadening can be surpassed by higher conversions at low flow rates.

Influence of reactor internal resistance.— Preconditioning operation in potentiostatic mode at 1.7 V, flow rate ratio $Q_{neg}/Q_{pos} = 3$, and positive flow rate of 10 µl/min was carried out in three different reactors with three different internal resistances (C1 = 211.4 Ω·cm², C2 = 62.6 Ω·cm², and C3 = 14.4 Ω·cm²) for a MVMRFB in which external electrical contacts of the reactor have been improved to reduce electrical resistance between external contacts and porous electrodes. $X_{VO^{2+}}$ was monitored via UV-vis spectroscopy with a total operation time of 60 min.

The graph in Figure 5 depicts the progression of the preconditioning operation with time. As the internal resistance decreases (higher power density), a higher $X_{VO^{2+}}$ can be attained. Employing a lower internal resistance value leads to a more rapid completion of the preconditioning process. Diminishing external contacts electrical resistance is directly related to higher current densities (as shown in Figure S6), as a result, the electrode experiences a higher rate of conversion of species.

Nevertheless, Figure 6 shows efficiency extracted at a fixed $X_{VO^{2+}}$ value of 75%. Processes with lower internal resistance achieving higher conversion will have a smaller number of reagents in the electrodes to convert. This will be related to small values of efficiency. Therefore, they are not compared at final operation time. For $X_{VO^{2+}} = 75\%$ efficiency achieves a maximum value of 54% for C2, and C3 achieves a smaller efficiency of 50%, since introducing a high number of electrons, due to higher current density, does not imply that they will find available species to react at the electrodes surface. Thus, part of these electrons is not converted to V^{3+} and VO^{2+} and could be used for side reactions. Moreover, these efficiencies could also be affected by ohmic losses at higher current densities and lower resistances, in addition to possible side reactions.

Therefore, although low reactor internal resistances can achieve preconditioning faster, it could be less efficient. A balance between preconditioning required time and efficiency must be considered.

Influence of side reactions. As anticipated in the previous section, operating at higher power density may lead to decreased efficiencies due to side reactions, mainly hydrogen

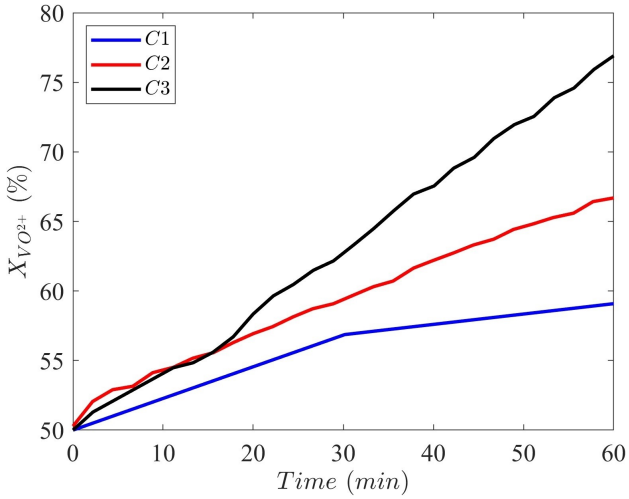

Figure 5. Influence of reactor power density in $X_{VO^{2+}}$ for a preconditioning operation at constant 1.7 V with $Q_{neg}/Q_{pos} = 3$ ratio and positive flow rate of 10 µL/min.

Research Article
doi.org/10.1002/batt.202300367
Chemistry Europe
European Chemical Societies Publishing

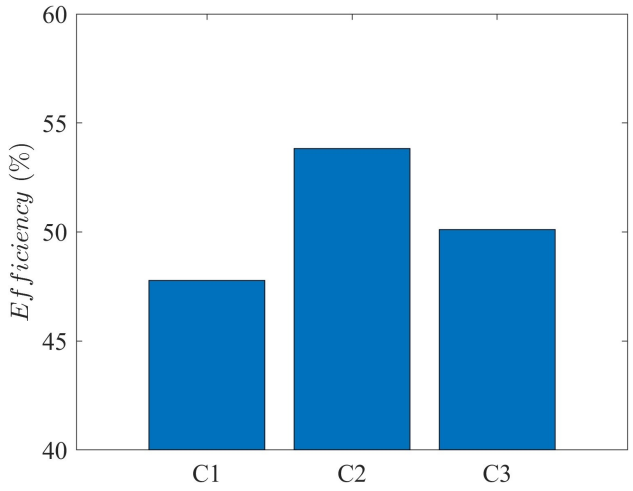

Figure 6. Efficiency for fixed $X_{VO^{2+}} = 75\,\%$ at three reactor internal resistances for preconditioning operation at constant 1.7 V with $Q_{neg}/Q_{pos} = 3$ ratio and positive flow rate of 10 μL/min.

and oxygen evolution,[29–31] taking place instead of vanadium redox reactions, due to higher current densities and higher overpotential. Due to absence of self-discharge during preconditioning operation, with species crossover by migration due to electric field being neglected and controlled only by diffusion, any imbalance that can be generated between the positive and negative sides must be evidence of side reactions occurring.

A preconditioning operation at the optimal flow rate ratio $Q_{neg}/Q_{pos} = 3$, $Q_{pos} = 10$ μl/min, with a reactor internal resistance of 62.6 $\Omega \cdot cm^2$ is carried out in potentiostatic mode at different cell potentials for 2.5 h. In order to evaluate the imbalance between $X_{VO^{2+}}$ and $X_{V^{3+}}$, both values are continuously monitored in real time via UV-vis spectrometer. Figure 7 shows the measured percentages as a function of time for applied voltages of 0.8 V, 1.2 V, 1.5 V, and 1.7 V. The corresponding current densities are presented in Figure S7. The magnitude of these voltages implies that oxygen evolution is avoided, leaving only hydrogen evolution reaction.[26]

The $X_{V^{3+}}$ tends to be lower than $X_{VO^{2+}}$, especially at higher voltages, resulting in the appearance of an imbalance between the electrolytes. Slower reaction rates are in the negative electrode, then to compensate reactions in the positive electrode, hydrogen side reaction can take place in negative side. In that way, the $X_{VO^{2+}}$ can still increase while the $X_{V^{3+}}$ remains the same, creating an imbalance. Operation at lower preconditioning voltage (e.g., 0.8 V) could suppress side reactions due to the absence of imbalance at 2.5 h.

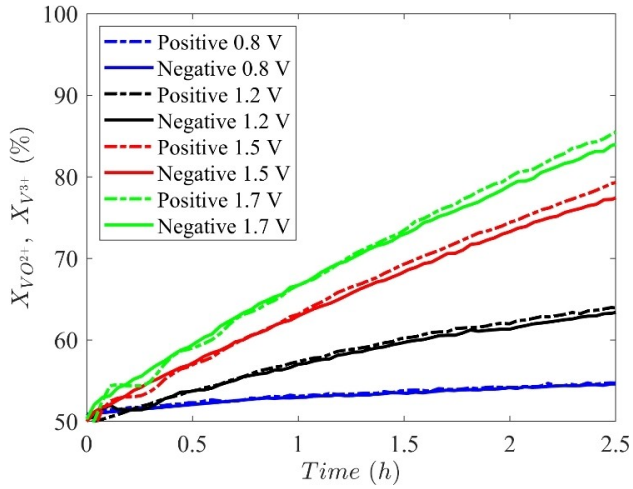

Figure 7. Influence of side reactions for a 62.61 Ωcm^2 reactor internal resistance, operating in potentiostatic mode at different voltages with flow rate ratio $Q_{neg}/Q_{pos} = 3$ and positive flow rate of 10 μL/min.

Conclusions

The present study provides new insights on the preconditioning operation of MVMRFBs in closed-loop recirculation operating mode. The MVMRFBs are operated with an automated closed-loop control, using micro actuators and micro flowmeters that enabled fine control of the flow rate, in order to operate during the entire preconditioning process with high stability. Preconditioning process evolution was determined by real time measurements of species concentration by UV-vis spectroscopy through 3D printed micro flow cuvettes.

Influence of negative to positive flow rate ratio was studied for MVMRFB, obtaining an optimum value of $Q_{neg}/Q_{pos} = 3$ for preconditioning operation. Using the optimal ratio, it was shown that operating at lower flow rates can improve performance due to an optimal relation between conversion in electrodes, current density, and efficiencies, achieving VO^{2+} concentrations of 88 % in positive electrolyte with an efficiency of 41 % after 7 h of process.

The influence of the reactor internal resistance was considered, demonstrating that low values of internal resistance (higher power densities) can yield inefficient processes as a product of species renovation due to laminar flow. Finally, thanks to the real-time dual UV-vis measurements, preconditioning imbalance between negative and positive electrolytes, product of side reactions, was monitored, showing that voltages higher than 0.8 V tend to generate side reactions as hydrogen in negative side, which allows to achieve preconditioning faster in the positive electrolyte than in the negative one. Imbalance due to side reactions emphasizes the need of sensors tracking concentrations of species in real time for MVMRFBs if a proper operation must be achieved, because an offset between electrolytes means capacity losses for the battery.

This work should be considered as a first step toward an operation protocol for the first charge-discharge process in a MVMRFB in recirculation mode. With an optimum preconditioning process, in the absence of an offset between positive and negative sides, a stable condition (separated species V^{3+} and VO^{2+}) for the MVMRFB will be achieved and charge-discharge cycling processes could be evaluated.

Experimental Section

Materials and setup.— Briefly, the membraneless micro reactor design used in this study is based on the Goulet et al.[32] Y-junction cell configuration with porous electrodes, designed to have two inlets and two separate outlets to operate in continuous recirculation mode. Electrolytes were pumped to the microfluidic reactor by an automated flow rate control including piezoelectric micro pumps and micro flowmeters. In this setup, the tanks were not included, and the electrolyte was continuously recirculated through the micro reactor.

3D printed inline micro flow cuvettes were installed at the outlet of reactor and connected to optical fibers, allowing to measure the optical absorbance of the electrolytes. By utilizing UV-vis spectrophotometer and following the procedure outlined in Section S1 of the Supporting Information, it becomes feasible to ascertain the molar fraction of VO^{2+} ($X_{VO^{2+}}$), presented as percentage using Equation S2.

Complete information about the cell design and fabrication, assembly of the system, control, and integration of the microfluidic system, as well as the procedure followed for spectrometer calibration, can be found in Section S1 of the Supporting Information.

Supporting information

The authors have cited additional references within the Supporting Information.[32–34]

Acknowledgements

This work was supported in part by the Industrial Doctorate Program of the Comunidad de Madrid under Grant IND2017/AMB-7719.

Conflict of Interests

The authors declare no conflict of interest.

Data Availability Statement

The data that support the findings of this study are available in the supplementary material of this article.

Keywords: microreactors · electrochemistry · vanadium · UV/vis spectroscopy · energy conversion · membraneless · redox flow battery · flow rate · side reaction

[1] C. F. Schleussner, J. Rogelj, M. Schaeffer, T. Lissner, R. Licker, E. M. Fischer, R. Knutti, A. Levermann, K. Frieler, W. Hare, *Nat. Clim. Change* **2016**, *6(9)*, 827–835.
[2] W. Kangro, H. Pieper, *Electrochim. Acta* **1962**, *7*, 435–448.
[3] M. Skyllas-Kazacos, M. Rychcik, R. G. Robins, A. G. Fane, M. A. Green, *J. Electrochem. Soc.* **1986**, *133*, 1057–1058.
[4] J. Noack, N. Roznyatovskaya, C. Menictas, M. Skyllas-Kazacos, in *Energy Storage News*, **2019**.
[5] W. Wang, Z. Nie, B. Chen, F. Chen, Q. Luo, X. Wei, G. G. Xia, M. Skyllas-Kazacos, L. Li, Z. Yang, *Adv. Energy Mater.* **2012**, *2*, 487–493.
[6] S. Kim, E. Thomsen, G. Xia, Z. Nie, J. Bao, K. Recknagle, W. Wang, V. Viswanathan, Q. Luo, X. Wei, A. Crawford, G. Coffey, G. Maupin, V. Sprenkle, *J. Power Sources* **2013**, *237*, 300–309.
[7] Z. Yang, J. Zhang, M. C. W. Kintner-Meyer, X. Lu, D. Choi, J. P. Lemmon, J. Liu, *Chem. Rev.* **2011**, *111*, 3577–3613.
[8] H. Vafiadis, M. Skyllas-Kazacos, *J. Membr. Sci.* **2006**, *279*, 394–402.
[9] Q. C. Jiang, J. Li, Y. J. Yang, Y. J. Ren, L. Dai, J. Y. Gao, L. Wang, J. Y. Ye, Z. X. He, *Rare Met.* **2023**, *42*, 1214–1226.
[10] Y. Jiang, Z. Liu, Y. Lv, A. Tang, L. Dai, L. Wang, Z. He, *Chem. Eng. J.* **2022**, *443*, 136341.
[11] M. L. Perry, R. M. Darling, R. Zaffou, *ECS Trans.* **2013**, *53*, 7.
[12] R. Zaffou, W. N. Li, M. L. Perry, *ACS Symp. Ser.* **2012**, *1096*, 107–127.
[13] M. Skyllas-Kazacos, *J. Power Sources* **2003**, *124*, 299–302.
[14] C. Sun, E. Negro, A. Nale, G. Pagot, K. Vezzù, T. A. Zawodzinski, L. Meda, C. Gambaro, V. Di Noto, *Electrochim. Acta* **2021**, *378*, 138133.
[15] A. F. Molina-Osorio, A. Gamero-Quijano, P. Peljo, M. D. Scanlon, *Curr. Opin. Electrochem.* **2020**, *21*, 100–108.
[16] P. Navalpotro, J. Palma, M. Anderson, R. Marcilla, *Angew. Chem.* **2017**, *129*, 12634–12639.
[17] M.-A. Goulet, O. A. Ibrahim, W. H. J. Kim, E. Kjeang, *J. Power Sources* **2016**, DOI 10.1016/j.jpowsour.2016.11.053.
[18] J. Marschewski, P. Ruch, N. Ebejer, O. Huerta Kanan, G. Lhermitte, Q. Cabrol, B. Michel, D. Poulikakos, *Int. J. Heat Mass Transfer* **2017**, *106*, 884–894.
[19] O. A. Ibrahim, M. Navarro-Segarra, P. Sadeghi, N. Sabaté, J. P. Esquivel, E. Kjeang, *Chem. Rev.* **2022**, *122*, 7236–7266.
[20] J. P. Esquivel, P. Alday, O. A. Ibrahim, B. Fernández, E. Kjeang, N. Sabaté, *Adv. Energy Mater.* **2017**, *7*, DOI 10.1002/aenm.201700275.
[21] M. A. Modestino, D. Fernandez Rivas, S. M. H. Hashemi, J. G. E. Gardeniers, D. Psaltis, *Energy Environ. Sci.* **2016**, *9*, 3381–3391.
[22] S. E. Ibáñez, A. E. Quintero, P. A. García-Salaberri, M. Vera, *Int. J. Heat Mass Transfer* **2021**, *170*, 121022.
[23] R. Ferrigno, A. D. Stroock, T. D. Clark, M. Mayer, G. M. Whitesides, *J. Am. Chem. Soc.* **2002**, *124*, 12930–12931.
[24] E. Kjeang, J. McKechnie, D. Sinton, N. Djilali, *J. Power Sources* **2007**, *168*, 379–390.
[25] E. Kjeang, R. Michel, D. A. Harrington, N. Djilali, D. Sinton, *J. Am. Chem. Soc.* **2008**, *130*, 4000–4006.
[26] J. W. Lee, M. A. Goulet, E. Kjeang, *Lab Chip* **2013**, *13*, 2504–2507.
[27] T. Sukkar, M. Skyllas-Kazacos, *J. Membr. Sci.* **2003**, *222*, 235–247.
[28] V. Muñoz-Perales, S. Berling, E. García-Quismondo, P. A. García-Salaberri, J. Palma, M. Vera, S. E. Ibáñez, *J. Electrochem. Soc.* **2022**, *169*, 100522.
[29] A. Fetyan, G. A. El-Nagar, I. Lauermann, M. Schnucklake, J. Schneider, C. Roth, *J. Energy Chem.* **2019**, *32*, 57–62.
[30] C. N. Sun, F. M. Delnick, L. Baggetto, G. M. Veith, T. A. Zawodzinski, *J. Power Sources* **2014**, *248*, 560–564.
[31] L. Wei, T. S. Zhao, Q. Xu, X. L. Zhou, Z. H. Zhang, *Appl. Energy* **2017**, *190*, 1112–1118.
[32] M. A. Goulet, E. Kjeang, *Electrochim. Acta* **2014**, *140*, 217–224.
[33] A. B. De Quirós, A. E. Quintero, A. Francés, A. A. Maurice, J. Uceda, *IEEE Access* **2023**, *11*, 46132–46143.
[34] P. Loktionov, R. Pichugov, D. Konev, M. Petrov, A. Pustovalova, A. Antipov, *J. Electroanal. Chem.* **2022**, *925*, 116912.

Manuscript received: August 25, 2023
Revised manuscript received: October 24, 2023
Accepted manuscript online: October 25, 2023
Version of record online: November 20, 2023